Unique Axial Flux Motor Design Delivers Superior Torque Density

Yong-Bae Jung PhD, Tom Long PhD, John Nelson PE, Christopher Landon ME
Apex Drive Laboratories Inc. 625 NW 17th Ave., Portland, OR, USA – www.apexdrivelabs.com

EET-2008 European Ele-Drive Conference
International Advanced Mobility Forum
Geneva, Switzerland, March 11 – 13, 2008

Abstract
The electric motor designed by Apex Drive Laboratories, Inc. represents a new class of axial flux permanent magnet (AFPM) machines. With its double-stator-single-rotor configuration and segmented U-shaped cores, the Apex motor achieves superior torque density in comparison to conventional AFPM and radial flux permanent magnet (RFPM) machines. The Apex motor is highly suited for the application of direct-drive systems.

Keywords: permanent magnet motor, NEV, finite element calculation, torque, flux saturation, axial flux

1 Introduction

In electric vehicle applications, the use of direct-drive motors is desirable because of the elimination of gear reducing differentials and transmissions. Some advantages of this are reduction of the vehicle cost and weight, higher reliability, and an increase of the total system efficiency. In consideration of the high-torque operation required at relatively low speeds, permanent magnet (PM) motors are best fit to the direct-drive application.

It is widely recognized that axial flux permanent magnet (AFPM) machines usually have higher torque densities and efficiencies than their radial flux (RFPM) counterparts. Its pan-cake shape geometry and high torque capability make AFPM motors a preferred choice for direct-drive systems. In recent years, many different topologies of AFPM machines have been developed and reported [1].

Apex Drive Laboratories has developed a new type of AFPM machine with segmented U-shaped cores that has higher torque density than conventional motor topology. One application of this motor is for the direct drive of a neighborhood electric vehicle (NEV). In this paper, the Apex AFPM motor topology is described and the analyses of motor performance through the use of Finite Element Analysis (FEA) techniques are presented. Test results from a proof of concept prototype are also presented.

2 Apex AFPM Motor Design

The Apex AFPM motor relies on two separate stators with salient cores made of low-loss grain-oriented magnetic material to complete the electromagnetic circuits. These circuits are used to rotate the single composite rotor which is populated with NdFeB permanent magnets. The use of disk-shaped magnets produces a sinewave back-EMF in this application. Figure 1 shows the details of a developed Apex AFPM motor.

The specifications of a motor created for the NEV application are shown in Table 1. This particular NEV uses two motors in place of the mechanical differential to provide traction while allowing the tires to spin at different speed, enabling the vehicle to navigate turns and un-even terrain.

Figure 1: Apex AFPM motor

Table 1: Apex motor spec for direct-drive NEV

Battery voltage	288	(V)
Starting torque	60	(Nm)
Peak torque	260	(Nm) at 550 rpm
Motor current	60	(A) cont. / 300 (A) peak
Outer Diameter	11.2	(inch)
Length	5.1	(inch)

2.1 Torque density

Torque density is the amount of torque produced by a given volume of motor. Torque density (σ) of a conventional electric motor can be expressed as the product of electric loading (A_c) and magnetic loading (B_m):

$$\sigma = A_c \cdot B_m \ \ [Nm/m^3]. \quad (1)$$

A fair comparison of the performance of motors can be made by studying how they produce torque. In all permanent magnet motors, electromagnets on the stator are energized in sequence so that the rotor chases after them. Taking a macroscopic approach, where torque is related to winding back-EMF through the use of conservation of energy principles, a general torque expression for a motor can be expanded as:

$$T = R \cdot A_g \cdot B_m \cdot N \cdot n_c \cdot I \ / \ \tau_p \quad [Nm], \quad (2)$$

where A_g is the cross sectional area of the air gap, B_m is the air gap flux density created by the magnets, n_c is the number of turns, I is the rated winding current, and τ_p is the pole pitch.

For conventional radial motors, R is the radius from the center of rotation to the center of the air gap between the magnets and the stator, and N is the number of magnets. For the Apex motor, R is the radius from the center of rotation to the center of the magnets, and N is the number of segmented cores producing torque at any given instance.

2.2 Conventional vs. Apex Motor

2.2.1 Longer torque arm

In equation (2), R is the radius at which torque is produced for a given motor diameter. The Apex motor provides for a longer torque arm (R) which is a key factor that allows more torque to be produced within a set geometry

2.2.2 Maximizing electric and magnetic loading

A fundamental tradeoff between electric and magnetic loading exists in both radial and axial motor designs. For a given diameter, in order to apply more windings, slot area must increase and the amount of iron must decrease. Doing so forces the same amount of magnetic flux through a smaller amount of iron which causes the iron to saturate sooner. More iron in the motor usually means less room for turns of wire to create the magnetic field, resulting in decreased motor performance. In a slotted AFPM stator design, there is a limit of the increasing number of conductors in a given slot area. However, a slotless AFPM stator design has a lower value of flux density because of increased effective air gap length. Typically, slots for windings extend radially outward from the center of the motor, leaving windings at the inside radius severely constrained. The unique segmented flux path of the Apex motor topology minimizes this inherent problem. The open space of the cores can be made large, allowing for more wiring without restricting the area of the iron that passes the magnetic flux. The number of conductors around a segmented core can be maximized up to the magnetic and thermal limit.

2.3 Minimizing Core Loss and Weight

The stator uses standard U-shaped magnetic cores which reduces the length of the magnetic flux path and eliminates unnecessary yoke area in the stator, as shown in Figure 2 illustrating the flux paths of AFPM motors. Because of these improvements, core weight and core loss can be reduced. The geometry of the U-shaped cores allows conventional coil winding techniques to easily maximize the fill factor of coil.

2.4 High Torque at Low RPM

Apex has found that the optimum ratio in the number of circular magnets and U-shaped or C-shaped segmented cores is N+1: N for a general N phase system. This ratio is part of the US patent [3]. This would result in a ratio of 4:3 for a three phase system. The number of magnets that can be put in the rotor would be dependent on the size of the magnet and the diameter of the rotor, as well as the number of cores that can fit in the stator in order to maintain the ratio of N+1:N. The high pole count in Apex motors results in a lower maximum rpm but higher torque for a given electrical drive rate.

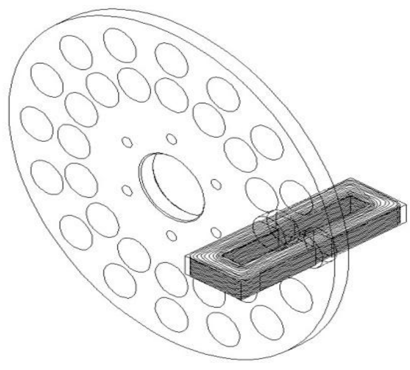

(a) Apex AFPM motor (single U-core shown)

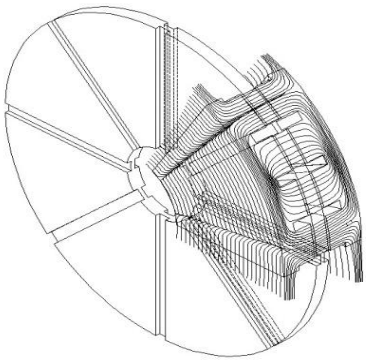

(b) Conventional AFPM motor (partial stator shown)

Figure 2: Flux path in AFPM motor

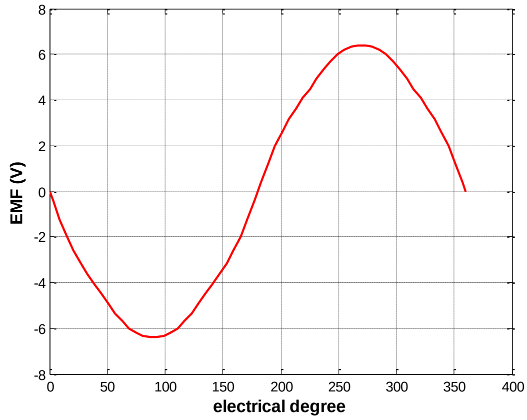

Figure 4: Calculated open circuit voltage at 100 rpm

3 Finite Element Analysis (FEA)

The initial size of a motor is determined using a design program based on a lumped parameter analysis of magnetic circuits. In order to refine the initial design, three dimensional magnetic Finite Element Analysis is performed. The effect of core saturation, harmonic contents in the back-EMF waveform, and reduction of cogging torque can be studied through this analysis.

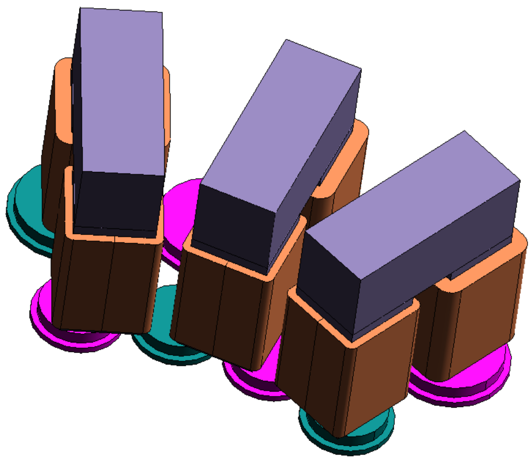

Figure 3: FEA model of Apex motor

Figure 3 shows the geometry for an FEA model using MagNet 3D package (Infolytica). Considering the symmetric and periodic conditions, a 1/10 size of the geometry is modeled. Flux linkage of stator winding is obtained and differentiated with respect to time to generate a back-EMF waveform. Simulations with 60 electrical degree span is enough because of periodicity in the A, B, and C phase. The size of the disk magnets is adjusted to reduce the harmonic components while still maintaining the torque constant of the motor. Figure 4 shows the calculated phase back-EMF waveform with a 3.5% harmonic distortion factor.

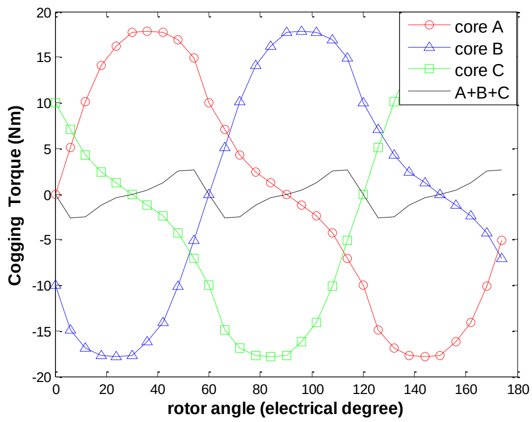

(a) Initial design

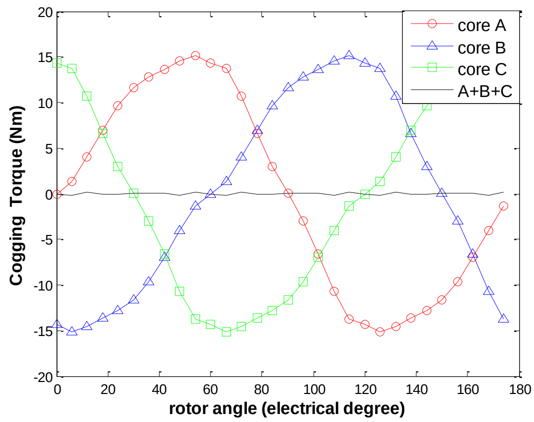

(b) Modified geometry

Figure 5: Cogging torque components

Several factors have an effect on the cogging torque of the Apex motor, including the magnet to core size ratio and skew angle between the inner and outer layer of magnets. Figure 5(a) shows cogging torque acting on phase A, B, and C cores. In this case, the net cogging torque of the motor has a dominant 6th harmonic component. By adjusting the geometry of the motor, the 6th harmonic component can be eliminated as shown in Figure 5(b).

Figure 6 shows excitation torque with different values of current. Developed torque is linearly proportional to the current up to two times the amount of rated current. Magnetic cores with a high saturation value are used to meet the requirements of peak torque performance for the NEV specifications.

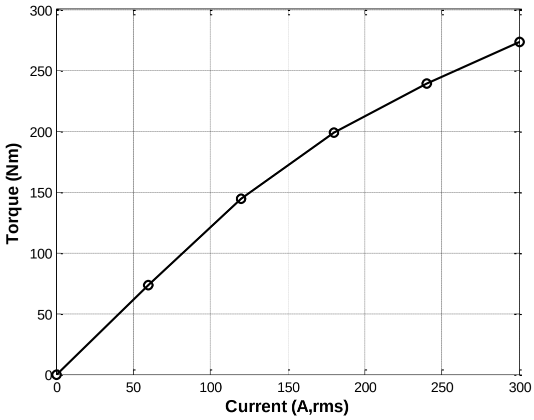

Figure 6: Torque saturation curve

4 Performance Calculation

Performance of PM synchronous motors can be calculated using phasor analysis [2]. Core loss is estimated from an open circuit rotational loss measurement. Motor parameters and effects of saturation obtained from 3D FEA calculation are used in the phasor analysis. Above base rpm, a flux weakening control scheme is used to overcome the increased back-EMF value.

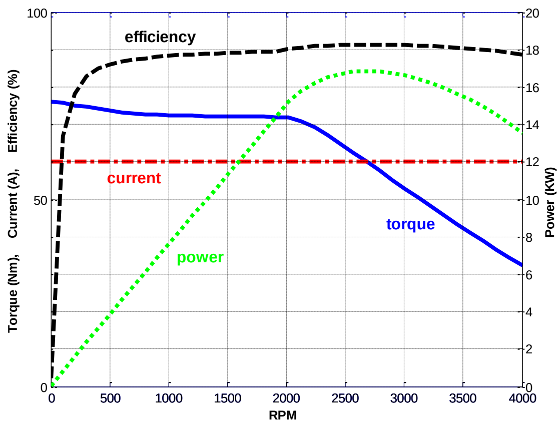

(a) Rated Current Condition

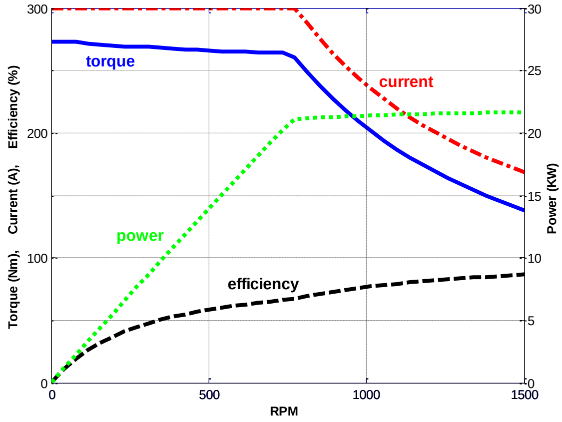

(b) Peak Current Condition

Figure 7: Apex motor performance curve

Although this NEV project only requires operation up to roughly 550 rpm, the developed Apex motor shows a high ratio between base and maximum rpm.

5 Prototype and Measurement

Currently, the custom designed controller for the NEV project is under development. The full load test results will be published in the future. However, test results from an early version of an Apex Proof of Concept (PoC) motor are presented in this paper. These tests were conducted at the Motor Systems Resource Facility at Oregon State University [6].

The motor was spun at constant rpm with a 21Volt sinusoidal three phase voltage source. A mechanical load (induction motor) was applied and current components were measured before losing synchronism.

Figure 8: Proof of Concept (PoC) motor under load test

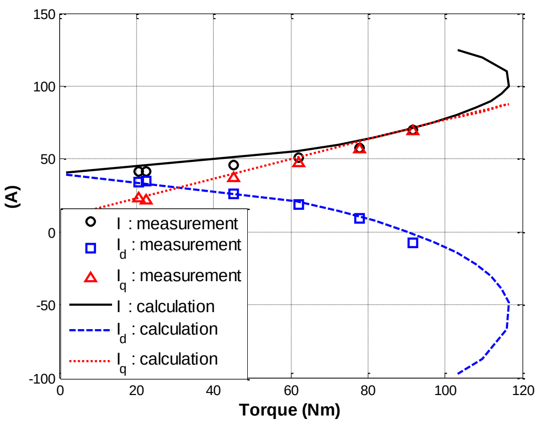

Figure 9: Measured and calculated current components of PoC motor in synchronous motor test

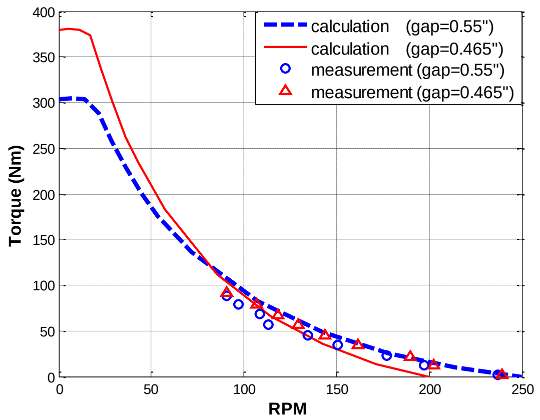

Figure 10: Measured and calculated torque of PoC motor

Figure 9 shows measured and calculated current components in *d-q* axis, and they agree well.

An off-the-shelf BLDC motor controller was used to spin the motor with a 72V battery. Figure 10 shows measured torque values at different rpm. The duty cycle of the controller output voltage was fixed to 67% with hard switching. Tests at low rpm were not accomplished due to the controller current limit. Using measured data from the PoC motor, final design of the Apex motor for the NEV application was completed, as shown in Figure 1.

6 Summary

The Apex AFPM motor presented in this paper has a higher torque density than other AFPM machines. Significant aspects of the machine design have been discussed and experimental results have been reported. FEA techniques have been used to accurately calculate the machine parameters. The novel arrangement of Apex AFPM machines results in very compact, light weight and efficient products, aspects which are required for the direct-drive applications. The Apex motor is protected by the patents [3]-[5].

Acknowledgments

The authors would like to thank Oregon State University for use of the MSRF laboratory and graduate student assistance.

References

[1] Aydin, M., S. Huang, T.A. Lipo, "Axial Flux Permanent Magnet Disc Machines: A Review," *Symposium on Power Electronics, Electrical Drives, Automation, and Motion (SPEEDAM)* 2004, pp.61-71, 2004

[2] T. J. E. Miller, *Brushless Permanent-Magnet and Reluctance motor Drives*, pp100 – 109, ISBN 0-19-859369-4, Clarendon Press, 1989.

[3] US 6,552,460B2 April 22, 2003 Brushless Electro-Mechanical Machine.

[4] US 6,930,433B2 August 16, 2005 Brushless Electro-Mechanical Machine.

[5] CIP 3.3 (Published February 2007) patent pending on the U-Core Design.

[6] Motor Systems Resource Facility at Oregon State University, http://eecs.oregonstate.edu/msrf/facility.html

Authors

Yong-Bae Jung received his PhD in Electric Power Engineering from Rensselaer Polytechnic Institute. He worked at R&D areas for Hyosung Corporation, Korea for 6 years. He is now a senior scientist at Apex Drive Laboratories, Inc. His has research interests in computational electromagnetics, design of electromagnetic devices and superconducting electric power apparatus.

Dr. Long holds an MBA from the University of Dayton, an AMP from Harvard University and a PhD from Portland State University. He worked as a senior manager for Tektronix and Planar Corporation. His education and career history have given him vast knowledge of logic, spectrum and network analyzers as well as expertise in software and electronic design systems.

John Nelson, PE has nearly seven years of dedicated mechanical engineering project management experience. With a B.S. from Washington State University, Mr. Nelson has former experience as a principle design engineer for Xerox Corporation with additional contract engineering projects including wind turbine gearbox designs and process systems for medical applications.

Christopher Landon, ME holds a BS in Engineering from Colorado School of Mines and is now a mechanical design engineer at ADL. He has previously worked as a mechanical engineer in the motion control industry on projects for gyro-stabilized camera systems as well as servo subsystems. He has gained a broad experience incorporating new technologies into products.